J Appl Electrochem (2007) 37:557–566
DOI 10.1007/s10800-006-9287-8

ORIGINAL PAPER

Electrocatalytic activity of copper alloys for NO_3^- reduction in a weakly alkaline solution

Part 2: Copper–tin

Z. Mácová · K. Bouzek · J. Šerák

Received: 3 March 2006 / Accepted: 11 November 2006 / Published online: 13 January 2007

Abstract A comparative study has been made of the influence of an addition of Sn to Cu as the basic cathode material on the electrocatalytic activity of the resulting material for nitrate (NO_3^-) reduction in a weakly alkaline medium. Potentiodynamic and chronoamperometric experiments were carried out in an electrolyte simulating the solution from regeneration of an ion-exchange column for NO_3^- removal in drinking water treatment. A rotating ring-disk electrode was used for these experiments. An enhancement of the electrocatalytic activity of Cu by alloying with Sn was observed only in the composition region up to 10 wt.% Sn. A further increase in Sn content results in a rapid decline of the electrocatalytic activity caused by changes in the phase structure of the alloy material. For the most active material potentiostatic batch electrolysis was carried out in a divided and an undivided cell. The reduction products were determined.

Keywords Nitrate · Electrochemical reduction · Copper · Tin · Electrocatalytic activity

Z. Mácová · K. Bouzek (✉)
Department of Inorganic Technology, Institute of Chemical Technology Prague, Technická 5, 166 28 Prague 6, Czech Republic
e-mail: bouzekk@vscht.cz

J. Šerák
Department of Metals and Corrosion Engineering, Institute of Chemical Technology Prague, Technická 5, 166 28 Prague 6, Czech Republic

1 Introduction

As well as causing environmental problems NO_3^- ions can also be hazardous to human health [1–3]. The occurrence of NO_3^- in subterranean and groundwater is mainly due to industrial waste and intensive agriculture. One of the most promising methods of NO_3^- removal from drinking water is ion exchange combined with electrochemical reduction [4, 5]. The present study is concerned with the electrochemical part of this process, the focus being on the alloy electrodes. These were found to display more suitable properties compared to pure metals.

In a weakly alkaline solution, the highest electrocatalytic activity was achieved using a Cu cathode [6], but NH_3 proved to be the final product. The application of binary or ternary alloys should lead to higher selectivity to N_2 as the final product and to an enhancement of the catalytic activity towards NO_3^- reduction. Various alloys have been investigated [7–17]. Sn or Cu combined with noble metals is often referred to as a suitable catalyst for NO_3^- reduction by H_2 [7–13]. The best polymetallic electrode materials for electrochemical reduction of NO_3^- are reported to be a Cu/Pd alloy [14] leading to N_2 as the final product, Ge-modified Pd [15] with N_2O and Sn-modified Pt with NH_3 and Pd/Au alloy [16, 17] with a mixture of N_2O and N_2 as the final products. These electrodes, however, have only been examined in acidic media.

The electrode material must be readily available and should have suitable mechanical properties, sufficient electrocatalytic activity and selectivity to N_2 as the final product. To date no material satisfying these requirements has been found. This is particularly true for weakly alkaline environments. The aim of this work is

to test the applicability of two types of economically viable alloys. In our previous work [1] Cu–Zn alloys were studied. A significant improvement in the reaction kinetics was observed compared to a Cu cathode. But reduction leads to NH_3 as the final product.

In the present work alloys of Cu and Sn are studied. A rotating ring-disk electrode (RRDE) was used to follow the electrocatalytic activity for NO_3^- reduction on bronzes with different Cu:Sn ratios and to compare it with pure Cu and Sn metals. The reaction products were determined for selected material by batch electrolysis.

2 Experimental

2.1 Chemicals

Solutions and chemicals identical to those used in [1] were also employed in the present study. The NO_3^- solution simulated the composition of the spent regenerant solution from the ion-exchange column filled with the anion exchanger Amberlite IRA 996 (Rohm and Haas, USA) with $-N^+Et_3$ functional groups located on an aromatic polymeric chain [4, 5]. It contained 84.0 g dm^{-3} $NaHCO_3$, 0.4 g dm^{-3} Na_2SO_4, 0.4 g dm^{-3} NaCl and 1.0 g dm^{-3} NO_3^- (in the form of $NaNO_3$). An artificial solution contaminated by NO_2^- (1.0 g dm^{-3} NO_2^- instead of NO_3^-) was studied in order to better understand the NO_3^- reduction mechanism. The background current was determined by measuring the polarisation curves in the blank solution of a supporting electrolyte without the addition of NO_3^- or NO_2^-.

The cathode materials were obtained in-house by alloying appropriate ratios of Cu and Sn. Alloys with the following Sn contents were prepared: 5, 10, 12, 30, 49 and 74 wt.%. These alloy compositions cover all phase structures formed by a Cu–Sn alloy [18]. The sample containing 30 wt.% Sn exhibits unsuitable mechanical properties. This material was too brittle and thus it was not possible to produce an electrode from it. The electrochemical catalytic behaviour of pure Cu and Sn was also studied for purposes of comparison.

The batch electrolyses were carried out with a bronze cathode containing 10 wt.% of Sn. The determination of NO_3^-, NO_2^- and NH_3 in the batch electrolyses was performed spectrophotometrically as described in [1].

2.2 Apparatus

The apparatus for the potentiodynamic measurements with a RRDE is described in detail elsewhere [1]. A standard three-electrode arrangement was used. The double wall cell temperature was controlled at 20 °C. Pt was the material used for both the counter-electrode and the ring electrode. SCE was used as a reference and all potentials in the text refer to this electrode. The initial potential for voltammetric experiments was chosen according to the open circuit potential (OCP) of the disk electrode in NO_3^- electrolyte. In the case of Sn and Cu, the initial potential was chosen slightly anodic (~20 mV) to OCP. Before each experiment the electrode was polarised at this potential for 20 s. Limited electrode dissolution and decomposition of possible copper hydride remaining on its surface was introduced by this means to ensure the reproducibility of the electrode surface after previous prolonged cathodic polarisation. In the case of alloy materials anodic polarisation was not applied before the experiments in an endeavour to avoid the selective dissolution of particular phases in the electrode structure. This process would lead to an undefined composition of the electrode surface at the start of the experiment. To ensure the copper hydride removal, electrode potential was held for 20 s at a value as anodic as possible, but still under slight cathodic polarisation against OCP. For all cathode materials a cathodic vertex potential was set at –1.80 V.

Additional chronoamperometric experiments were performed employing a Cu electrode and a bronze electrode with 10 wt.% Sn in order to understand the processes taking place at the electrode surface at potentials corresponding to peaks I and II. One experiment lasted 10 min. In order to ensure the reproducibility of the electrode surface and the resulting data the electrodes were potentiodynamically cycled before each experiment. The potential range of cycling was identical to the RRDE experiments (see above). The appropriate potentials for the potentiostatic experiments were chosen according to the cyclic voltammetry results.

In the first set of batch electrolysis experiments a flow-through undivided cell with a fluidised bed of inert particles in the inter-electrode space was employed (Fig. 1). Inert particles consisting of glass spheres 0.4–0.8 mm in diameter with a bed expansion of 50% were utilised for mass transfer enhancement and mechanical abrasion of the cathode surface. An iridium and tantalum oxide activated titanium anode (ATA) and bronze cathode, both with the dimensions 0.18×0.026 m^2, were positioned on the walls of the electrolyser. The temperature of the electrolyte was maintained at 20 °C by means of a thermostat. The hydrodynamic conditions of the electrolyses were the same as in [19]. Therefore identical transport parameters were considered: kinematic viscosity of the

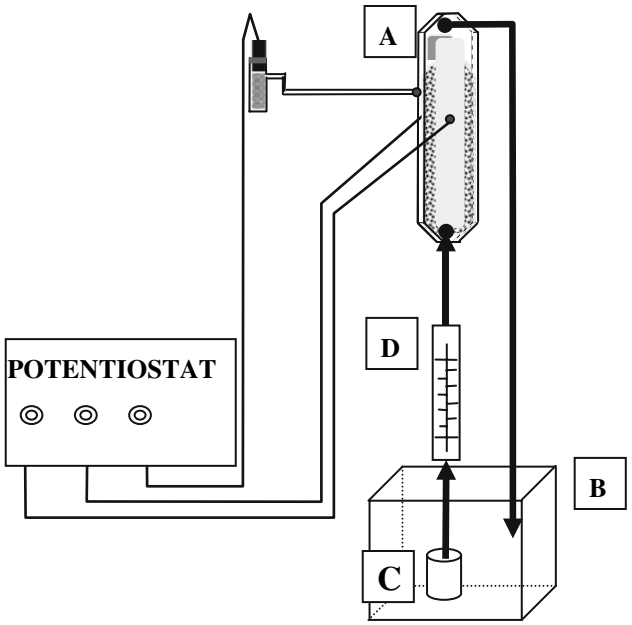

Fig. 1 Scheme of the batch electrolyser with a fluidised bed of inert particles. (**A**) flow-through electrolyser, (**B**) reservoir, (**C**) pump and (**D**) flow meter

electrolyte 1.193×10^{-6} m^2 s^{-1}, diffusion coefficients of the NO_3^- ion and O_2 1.9×10^{-9} m^2 s^{-1} and 2.3×10^{-9} m^2 s^{-1}, respectively.

In the second set of experiments the electrode compartments were separated by a PVC diaphragm. The anode compartment was filled with an electrolyte solution identical to that in the cathode compartment. In contrast to the latter it was not recirculated. A PVC diaphragm (Eilenburger Chemie-Werk GmbH., Germany) 0.65 mm thick with 43.4% porosity and a mean pore radius of 28 μm was used.

3 Results

3.1 RRDE experiments

The arrangement of experiments and data processing were performed in the same manner (elimination of the supporting electrolyte influence by subtracting the background current) as in [1], i.e. subtracted polarisation curves are presented throughout this work.

The Cu polarisation curve with a detailed specification of individual current peaks is given in the first part of this study [1]. It should be mentioned in that the Cu polarisation curve is characterised by three cathodic peaks corresponding to a reduction of NO_3^- to NO_2^- in the first step and a reduction of NO_2^- to NH_3 in the subsequent step. A layer of copper hydrides inhibiting NO_3^- reduction formed on the Cu electrode surface during polarisation at high cathodic potentials. This is confirmed by the fact that the current density of the NO_3^- reduction peaks in the reverse potential sweep is much lower in comparison to the initial cathodic sweep.

3.1.1 The Sn electrode

The subtracted potentiodynamic curve of the Sn rotating disk electrode (RDE) obtained for NO_3^- reduction is given in Fig. 2. No significant peak was observed. The current density increase starting at –1.35 V indicates the initiation of the reduction processes. The experiments with higher potential scan rates showed no clear peak.

The current response at the ring electrode (RE) held at 1.00 V indicates oxidisable products arising at the Sn disk electrode (DE) in the potential region –1.50 V to –1.80 V. A couple of current waves and peaks were observed on the response curve when the DE potential was shifted in the cathodic direction. Hysteresis of the current response in the reverse scan of the DE

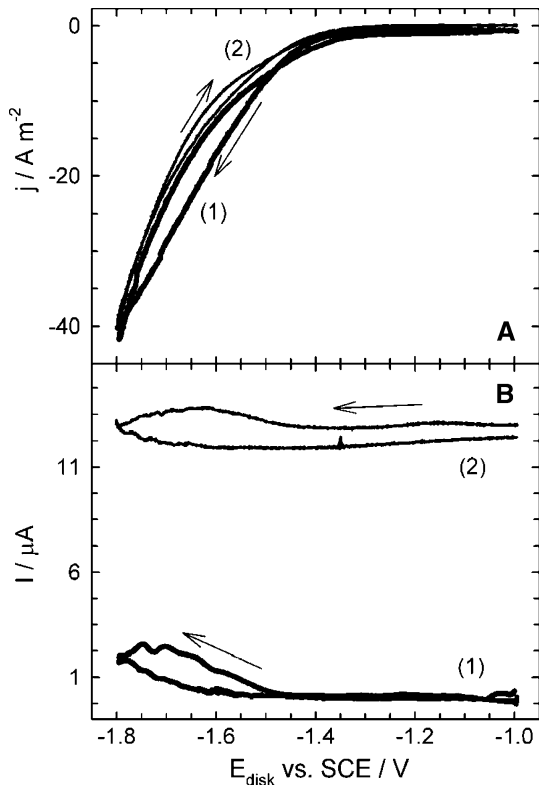

Fig. 2 (**A**) Subtracted potentiodynamic polarisation curve of a rotating Sn DE and (**B**) subtracted related current response of a Pt RE at a potential of 1.00 V. The electrolyte solution used: (1)—NO_3^- and (2)—NO_2^-; DE potential scan rate 10 mV s^{-1}, electrode rotation rate 20 Hz. The arrows indicate the DE potential scan direction

potential was observed. In accordance with previous results [6], this indicates NH_3 production at the cathodic vertex potential. Since NH_3 inhibits the Pt ring surface [6], the value of the current response is reduced substantially.

When a lower potential was applied to the RE (0.80 V), the responses changed but did not disappear (Fig. 3B). This clearly indicates intermediates oxidisable at 0.80 V being produced at the Sn cathode. At 0.60 V the current response character changed significantly. The current peaks disappeared and the current response rose exponentially. This shows that the intermediates oxidised on the RE at two previous potentials are no longer participating in the oxidation reaction. They are most probably no longer adsorbed on the RE surface. On the bare RE surface the reoxidation of H_2 produced at the DE takes place. The reason for the current response being higher (Fig. 3 presents the subtracted curves) than in the blank electrolyte is not yet clear.

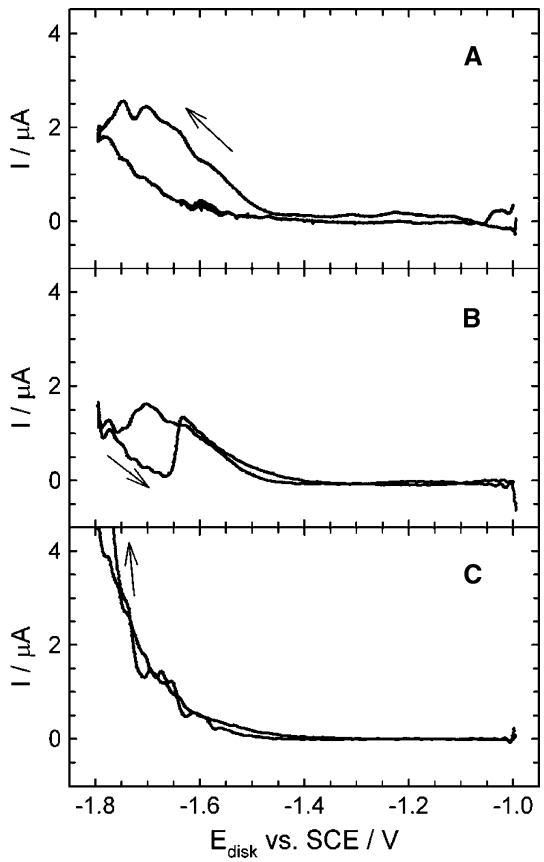

Fig. 3 Comparison of subtracted current response on a Pt RE at different potentials. Potentials used: (**A**) 1,000 mV, (**B**) 800 mV, (**C**) 600 mV. NO_3^- electrolyte solution, Sn DE potential scan rate: 10 mV s^{-1}, rotation rate 20 Hz

The DE potentiodynamic curve obtained in the NO_2^- solution exhibits only minor changes compared to the NO_3^- solution (see Fig. 2). The increase in current density is steeper and is slightly shifted cathodically.

The baseline of the current response of the RE has shifted to more anodic values because of the oxidation of NO_2^- ions present in the solution throughout the experiment. This effect is observed at all electrode materials under study. The relatively weak response increase in the potential region of the DE reaction corresponds to the reoxidation of reduction products brought from the DE to the RE electrode. It is important to note that the intensity of the RE current response is approximately one order of magnitude lower compared to the Cu experiments. The inhibition of the Pt RE surface by Sn ions that have drifted from the surface of the DE is a possible reason for this. This phenomenon was apparent at all electrode materials with Sn content higher than 10 wt.%.

3.1.2 The alloy of 5 wt.% Sn and 95 wt.% Cu

Significant changes in the Cu polarisation curve [1] were observed after addition of 5 wt.% Sn to Cu (Fig. 4). Three peaks, labelled I_{5Sn}, II_{5Sn} and III_{5Sn}, can be seen on the potentiodynamic curve. They are similar to the current peaks observed for the Cu electrode, see inset in Fig. 4 and detailed discussion in [1]. After reaching a well-defined current shoulder at a potential of –1.30 V the current density of the subtracted polarisation curve turns steeply towards anodic values. This is due to the inhibition of hydrogen evolution as a parasitic reaction in the presence of NO_3^- or NO_2^- ions and/or their reduction products. After subtracting a blank experiment this results in an apparently anodic current. The hysteresis of the curve in the anodic scan indicates inhibition of the electrode surface.

The current responses at the Pt RE to peaks I_{5Sn}, II_{5Sn} and III_{5Sn} are all well developed at a potential of 1.00 V. The response to peak II_{5Sn} vanishes at lower potentials; thus it probably corresponds to NO_2^- re-oxidation. This is confirmed by the II_{5Sn} peak missing on the polarisation curve recorded in the NO_2^- electrolyte. The current response to peak III_{5Sn} is cathodically shifted. There are two peaks that correspond to it, and of these only one is found in the RE response in NO_2^- electrolyte. This indicates that peak III_{5Sn} corresponds to a complex reaction mechanism that leads from NO_3^- to the final product. When experiments at a lower RE potential were carried out, the response to peak III_{5Sn} remained on the RE curve and reached even higher current values. A hysteresis of the RE curve in the anodic sweep again indicates

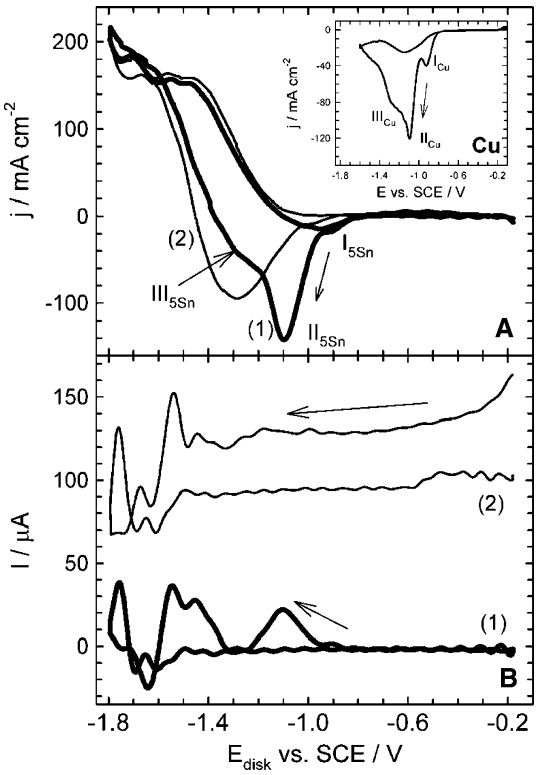

Fig. 4 (**A**) Subtracted potentiodynamic polarisation curve of a rotating bronze (5 wt.% Sn) DE and (**B**) subtracted related current response of a Pt RE at a potential of 1.00 V. (1)—NO_3^- and (2)—NO_2^-; DE potential scan rate 10 mV s^{-1}, electrode rotation rate 20 Hz. The arrows indicate the DE potential scan direction

inhibition of the Pt surface by NH_3 formed at the DE [6]. The current response in the NO_2^- experiment drops slightly in the proximity of the DE potential of –1.20 V, indicating the start of NO_2^- reduction on the DE and subsequent depletion of these ions.

3.1.3 The alloy of 10 wt.% Sn and 90 wt.% Cu

The behaviour of the bronze electrode with 10 wt.% of Sn in NO_3^- electrolyte is shown in Fig. 5. It is characterised by two significant peaks labelled I_{10Sn} at –0.90 V and II_{10Sn} at –1.12 V on the DE potentiodynamic curve. These two peaks are followed by a significant increase in current density in the potential region –1.20 V to –1.80 V. Increase in scan rate did not result in the detection of any new current peak. No hysteresis of the curve is apparent during the cathodic scan.

The highest current response of RE at 1.00 V corresponds to peak II_{10Sn}. Since this response is missing at lower RE potentials, peak II_{10Sn} can be ascribed to the reduction of NO_3^- to NO_2^-, similarly to the previous cases. This is further confirmed by the absence of this current peak in experiments with NO_2^--containing electrolyte.

The RE current response in the DE potential region of –1.20 V to –1.80 V is complex. This gives rise to the suspicion of experimental error. Nevertheless, a connection between the polarisation curve of the DE and the RE response is evident. It is clear that the complexity of the current response reflects the complicated mechanism of the reduction process. Particularly interesting is the absence of hysteresis in the RE response.

The disappearance of peak II_{10Sn} in the NO_2^- experiment (Fig. 5) caused the appearance of a new peak III_{10Sn} which had previously been overlapped. The higher scan rates did not reveal any other peak. It is unusual for the current density of NO_2^- to be lower than that of NO_3^- reduction. This indicates lower electrocatalytic activity of the electrode for NO_2^- reduction. With the exception of the missing response to peak II_{10Sn} the RE current response curve is qualitatively similar to that of the NO_3^- experiment.

The high current density observed on the DE polarisation curve at the cathodic vertex potential and the RE current responses to it resemble the behaviour of the Sn DE in this potential region.

3.1.4 The alloy of 12 wt.% Sn and 88 wt.% Cu

Peak II_{12Sn} on the potentiodynamic curve of bronze with 12 wt.% of Sn (Fig. 6) resembles peaks II_{10Sn} and II_{5Sn} ascribed to the reduction of NO_3^- to NO_2^-. This is confirmed by its disappearance during the NO_2^- experiment (see Fig. 6). Experiments conducted at higher scan rates revealed that peak II_{12Sn} overlaps another peak I_{12Sn} that resembles peaks I_{Cu}, I_{5Sn} and I_{10Sn}. It is missing on the polarisation curves of the NO_2^- experiments. At a DE potential of –1.25 V peak III_{12Sn} is well developed. As confirmed by the NO_2^- experiment it is connected with the reduction of NO_2^-.

An increase in current density was detected in the potential range –1.50 V to –1.80 V as in the case of 10 wt.% Sn bronze. During the NO_2^- experiment a new peak IV_{12Sn} developed at a potential of –1.70 V. Significant hysteresis during the anodic scan was observed for both the NO_3^- and NO_2^- solutions.

The current response of the RE to peaks I_{12Sn} and II_{12Sn} during the NO_3^- experiment was clearly detectable at 1.00 V and it disappeared at lower potentials. A well-developed current response to peak III_{12Sn} was also detectable at lower RE potentials.

In NO_2^- solution the RE response to peaks II_{12Sn} to IV_{12Sn} is visible. Due to the low signal level they are

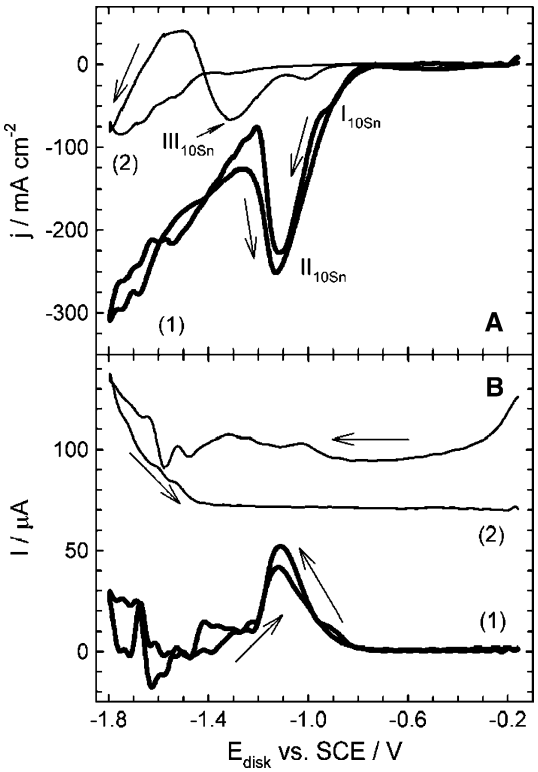

Fig. 5 (**A**) Subtracted potentiodynamic polarisation curve of a rotating bronze (10 wt.% Sn) DE and (**B**) subtracted related current response of a Pt RE at a potential of 1.00 V. (1)—NO_3^-, (2)—NO_2^-; DE potential scan rate 10 mV s^{-1}, electrode rotation rate 20 Hz. The arrows indicate the DE potential scan direction

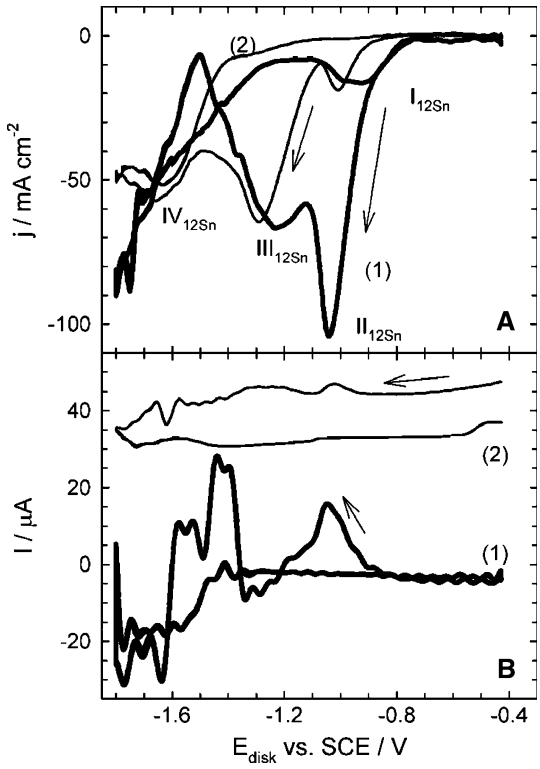

Fig. 6 (**A**) Subtracted potentiodynamic polarisation curve of a rotating bronze (12 wt.% Sn) DE and (**B**) subtracted related current response of a Pt RE at a potential of 1.00 V. (1)—NO_3^-, (2)—NO_2^-; DE potential scan rate 10 mV s^{-1}, electrode rotation rate 20 Hz. The arrows indicate the DE potential scan direction

not easily distinguished, but are noticed even at lower RE potentials.

The behaviour of bronze with 12 wt.% Sn resembles the sum of Cu and Sn.

3.1.5 Materials with higher Sn content

Potentiodynamic curves of materials containing 49 and 74 wt.% of Sn are not shown because their electrochemical behaviour was almost identical to that of pure Sn. This corresponds to [20], where the authors concluded that bronzes belonging to the composition range 60–100 wt.% of Sn produce a polarisation curve similar to that of pure Sn. In [20] NaOH solution was used as electrolyte. Nevertheless, their results are in agreement with our observations. The only exception is the material with 49 wt.% of Sn which, according to [20], behaves as if consisting of pure Sn and Cu independent of each other. This was not observed here.

3.2 Kinetics evaluation

Kinetics were evaluated in the same way as in [1]. The current peak corresponding to the reduction of NO_3^- to NO_2^- was chosen to compare the kinetics of the desired reaction for the individual cathode materials, i.e. peaks II_{Cu}, II_{5Sn}, II_{10Sn} and II_{12Sn}. Current density at a potential of –1.70 V, where NO_3^- reduction is assumed, was used for a kinetic evaluation of the Sn cathode. The Koutecky–Levich plots obtained exhibited good linearity. The only exception was the plot for bronze with 5 wt.% Sn, which showed a non-linear trend at high electrode rotation rates. The results of the Koutecky–Levich analyses are summarised in Table 1. The kinetics of NO_3^- reduction was found to be fastest at the bronze electrode with 10 wt.% Sn. Its electrocatalytic activity for NO_3^- reduction is nearly four times higher than that of the Cu electrode.

3.3 Chronoamperometry

All the polarisation curves of Cu and bronzes are characterised by a prominent peak labelled I. This was formerly considered to correspond to adsorption on Cu materials. Another explanation considered was the reduction of corrosion products following preconditioning of the electrode. However, the chronoamperometric experiments performed at the potential

Table 1 The kinetic current densities for the NO_3^- reduction determined by Koutecky–Levich analysis; for the bronze cathode materials the composition is given as a ratio of the weight percent of the individual components

	Cathode material				
	Cu	Sn	Cu:Sn = 95:5	Cu:Sn = 90:10	Cu:Sn = 88:12
j_k/A m^{-2}	–120	–50	–140	–455	–130

of this peak indicated a continuous Faradaic process related to NO_3^- reduction [1]. As shown in Fig. 7, this is also the case with bronze containing 10 wt.% Sn.

3.4 Batch electrolyses

The first set of experiments was performed in an undivided cell. Bronze containing 10 wt.% Sn was used as cathode. Figure 8 shows concentrations of compounds monitored during electrolyses at selected potentials.

The reduction of NO_3^- at –1.10 V and –1.30 V was conducted only to the stage of NO_2^-. A molar balance of N [1] indicated no formation of N-compounds other than NO_3^- or NO_2^-. After a certain time (~100 min) NO_2^- began to oxidise slowly back to NO_3^- at the anode. This is indicated by the fact that the concentration of NO_3^- and NO_2^- was almost constant with time.

At a potential of –1.50 V the situation differed: the NO_3^- reduction proceeded faster during the first 100 min and the NO_2^- concentration increased steeply. After that re-oxidation began and the NO_3^- concentration rose. At the 230th minute of electrolysis NO_3^- reduction was resumed and NO_3^- concentration declined again. As seen in Fig. 8, NH_3 is formed in the region of NO_2^- concentration decay, but it disappears when NO_3^- reduction resumes. Since the N-compound molar balance displays a deficit, N_2 is considered to be the final product of NO_3^- reduction.

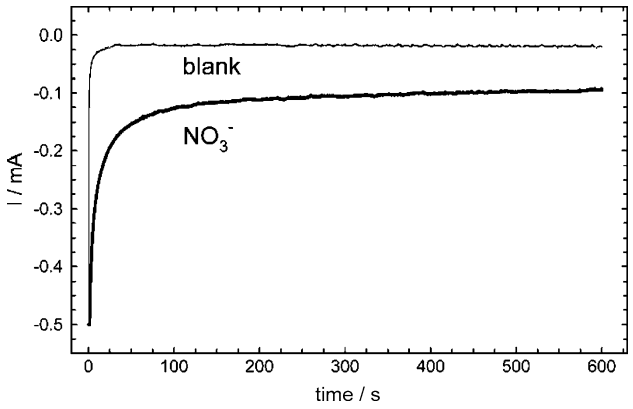

Fig. 7 Chronoamperometric curve of a stationary bronze electrode with 10 wt.% Sn in blank and NO_3^- electrolyte at a potential of –0.92 mV

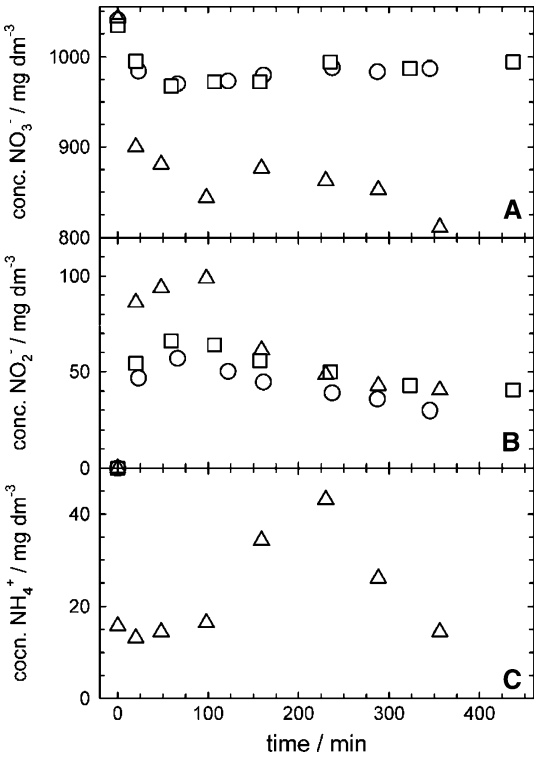

Fig. 8 The dependence of: (**A**) NO_3^-, (**B**) NO_2^-, (**C**) NH_3 concentrations on the duration of the batch electrolysis. Cathode potentials used: (○)—1.10 V, (□)—1.30 V and (Δ)—1.50 V

In the second set of experiments the cell was divided by a PVC diaphragm in order to minimise NO_2^- reoxidation at the anode. In Fig. 9 the results of an experiment at a cathode potential of –1.10 V are compared with those in an undivided cell. The NO_3^- concentration declined monotonically and the NO_2^- concentration reached correspondingly higher values. NH_3 first occurred after the NO_3^- concentration had been reduced to below 800 mg dm^{-3} and the concentration of NO_2^- exceeded 100 mg dm^{-3}. Afterwards its concentration slowly rose. The mass balance analysis of N-compounds indicates that NH_3 is not the only product—it corresponds to approximately 65% of the total molar amount of NO_3^- reduction products. No NH_3 was detected under similar conditions in experiments at –1.50 V in a divided cell. N_2 is assumed to be the only product.

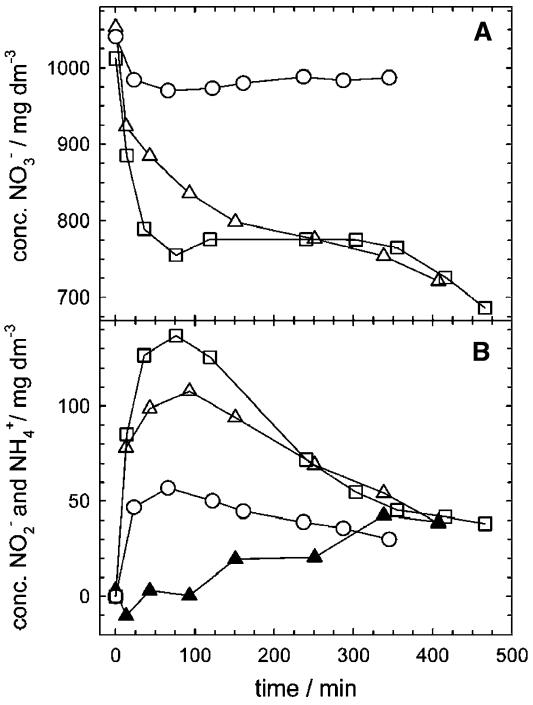

Fig. 9 Comparison of the batch potentiostatic electrolyses at –1.10 V in different cell arrangements. (**A**) NO_3^- concentration time dependence in an: ○—undivided and Δ—divided cell, □—electrolysis at –1.50 V in an undivided cell; (**B**) concentration–time dependence of: ○—NO_2^- in an undivided cell, Δ—NO_2^- in a divided cell, □—NO_2^- in an undivided cell at –1.50 V, ▲—NH_3 in a divided cell

4 Discussion

4.1 RRDE experiments

In NO_3^- solution the polarisation curves of bronzes with low Sn content (up to 15%) exhibit two peaks equal to I_{Cu} and II_{Cu} marked in Figs. 4–6 as I_{xSn} and II_{xSn}, where x is 5, 10 or 12. There is a corresponding response on the RE, indicating the reduction of NO_3^- to NO_2^- at the DE. This statement is also supported by the fact that these peaks practically vanished in the NO_2^- electrolyte. This means that in this potential region Cu plays a major role in the reaction mechanism.

Whereas the behaviour of the bronze with 5 wt.% Sn in principle still resembles that of pure Cu [6], the bronzes with 10 wt.% and 12 wt.% Sn differ significantly. The polarisation curves indicate significant changes in the reaction mechanism compared to the Cu cathode, e.g. the absence of the RE current response hysteresis indicates that no intensive NH_3 formation takes place at the DE. In particular, an alloy with 10 wt.% Sn exhibits outstanding properties, e.g. no hysteresis, which is certainly connected with the low sensitivity of this material to inhibition by Cu hydrides. According to Koutecky–Levich analysis it also has the highest electrocatalytic activity towards NO_3^- reduction.

The metallographic structure of the materials studied may supply an explanation. According to the literature [18], the Cu–Sn alloy consists of a single phase in the equilibrium region of 0.0–15.8 wt.% Sn. It contains solid solution α in which Sn is homogeneously dispersed. Nevertheless in the composition region 11.0–15.8 wt.% Sn an additional phase δ containing 31.0–33.5 wt.% of Sn homogeneously mixed with Cu can also appear in the structure. This is caused by the preparation method, e.g. by annealing. The amount of the eutectoid mixture of α + δ ($Cu_{31}Sn_8$) then increases with increasing Sn content. A metallographic analysis of bronze samples used was performed. The individual grains of α solid solution are detectable on metallographic scans of bronze samples with 5 wt.% and 10 wt.% Sn (Fig. 10A, B). In contrast, regions of eutectoid α + δ on the borders of α solid solution grains were observed in the sample with 12 wt.% Sn (Fig. 10C)—the base of the eutectoid consists of δ phase (bright areas) and the fine structure of phase α (darker areas) is located in it.

It may be assumed that only an increase in Sn content in the α phase leads to enhancement of the electrocatalytic activity of bronze towards NO_3^- reduction. Formation of δ phase with higher Sn contents causes its rapid decline. This was confirmed by experiments with bronzes with a higher Sn content (49 wt.% and 74 wt.%).

Similarly to brasses [1], in the case of bronze alloys, Cu participates in NO_3^- reduction, mainly in the region of lower potentials and the second metal (here Sn) does not assert itself, except for kinetic enhancement, until higher cathodic potentials are reached.

4.2 Batch experiments

Contrary to expectation, the batch electrolyses with a 10 wt.% Sn bronze cathode did not lead to fast NO_3^- removal. The current efficiency in an undivided cell at –1.10 V was about 15% and at –1.50 V it was almost the same. The separation of the electrode compartments by a diaphragm increased the current efficiency during electrolysis at –1.10 V to 40%, at –1.50 V it remained at 15%. An analysis of the contributions of individual processes in the reactor was made.

The reduction of O_2 consumes part of the current. The limiting current density of O_2 reduction under conditions similar to those used in the present study has a value of 4.1 A m^{-2} [19]. Taking into account the

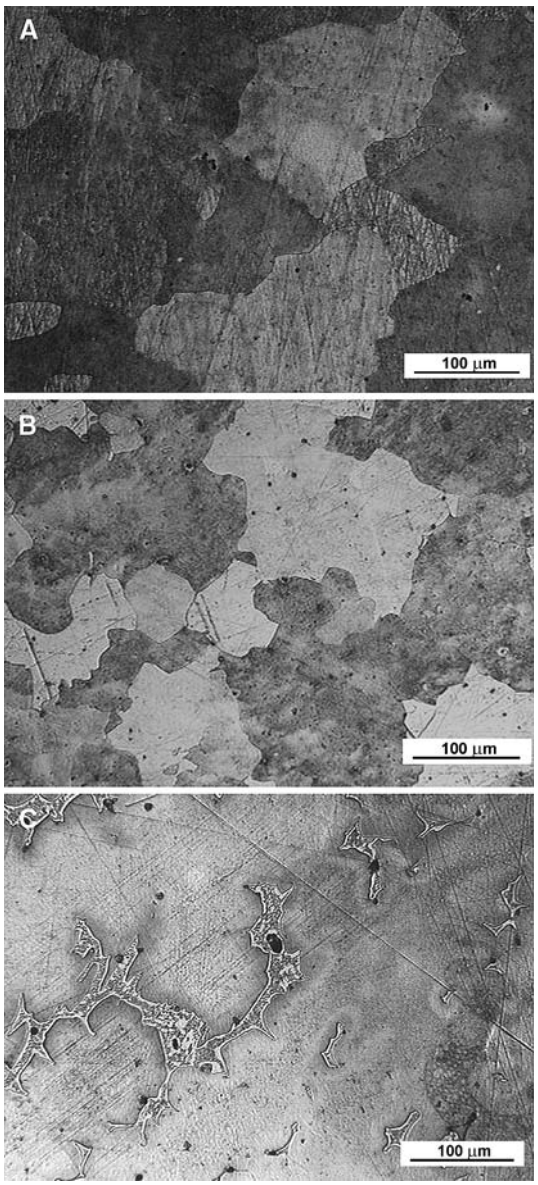

Fig. 10 Metallographic scan of bronzes: (**A**) 5 wt.% Sn, (**B**)10 wt.% Sn, (**C**) 12 wt.% Sn. Etching agent: 0.2 mol dm^{-3} $FeCl_3$ in 0.2 mol dm^{-3} HCl solution

total current density measured at –1.10 V (33.0 A m^{-2} on average) this represents approx. 15 %. In the case of electrolysis at –1.50 V (220.0 A m^{-2} on average) this represents less than 2%. Thus NO_3^- and O_2 reduction consumes 30% and 17% of total current during electrolysis at –1.10 V and –1.50 V respectively.

The last option, except for H_2 evolution as a parasitic reaction, is the reoxidation of NO_2^-. Conditions similar to those in [19] were considered, when the limiting current density of NO_2^- reoxidation was evaluated. During electrolysis performed at –1.10 V, NO_2^- concentration achieved a value of 56 mg dm^{-3}. The limiting current density corresponding to this concentration has a value of 8.2 A m^{-2}. Thus if NO_2^- reoxidation proceeds under mass transfer control, the current efficiency of NO_3^- reduction is in reality by 25% higher than that determined experimentally. That is the percentage of total current density used for immediate reoxidation of NO_2^- produced at the cathode to NO_3^-. In the case of electrolysis at –1.50 V (98 mg dm^{-3}) NO_2^- re-oxidation gave 14.4 A m^{-2}, i.e. the real reduction efficiency of NO_3^- is by 7% higher. This is in agreement with the results at –1.10 V. Here the separation of the electrode compartments, and thus the avoidance of NO_2^- reoxidation, resulted in an increase in current efficiency of batch electrolysis from 15 to 40%, i.e. by 25%. At –1.50 V no increase in current efficiency was observed. This is due to the prevailing effect of hydrogen evolution as a parasitic reaction and direct reduction of NO_3^- to a final product at a high cathodic potential.

The previous discussion can be summarised as follows: NO_3^- reduction itself consumes 40% and 22% of total current during electrolysis at –1.10 V and –1.50 V respectively. At the same potentials oxygen reduction represents 15% and 2% respectively of the total current. The hydrogen evolution reaction thus consumes approximately 45% and 76% respectively of the electrical charge. These values are substantially higher than those obtained from the voltammetric experiments. The reason for the discrepancy between RRDE and batch experiments may arise from changes in surface electrode composition. XRF analysis was performed to verify this theory, but it did not reveal differences between a fresh bronze surface and a surface after ten electrolyses. Another aspect is the electrolyte solution composition. Whereas in the case of the RRDE experiments the composition of the solution was well defined, in the case of batch electrolysis it changed substantially during the first minutes of electrolysis. This is due to the different ratio of electrode surface area to electrolyte volume in the two experimental arrangements.

5 Conclusion

The positive effect on electrocatalytic activity of addition of Sn to Cu as a base cathode material was observed in the composition region of up to 10 wt.% Sn. A further increase in Sn content led to a rapid decline in activity. This was explained in terms of the development of a new phase of eutectoid $\alpha + \delta$. The selectivity of the cathode material to the final product was affected only at highly cathodic potentials (more

cathodic than ~–1.40 V), where a product different from NH_3 (probably N_2) was indicated. However, the efficiency of this process was very low because hydrogen evolution is the prevailing process in this potential region. Additionally, the re-oxidation of NO_2^- on the anode surface represents a serious problem in the case of undivided cells and low cathodic potentials.

Acknowledgements Financial support by the Ministry of Education, Youth and Sports of the Czech Republic under project number CEZ: MSM6046137301 and by the Grant Agency of the Czech Republic under the project number 104/05/0066 is gratefully acknowledged.

References

1. Mácová Z, Bouzek K (2005) J Appl Electrochem 35:1203
2. Linberg R (1998) Artif Cell Blood Sub 26:133
3. Ullmann's Encyclopaedia of Industrial Chemistry, 6th edn., Nitrates and Nitrites, Chapter 10 – Toxicology and Occupational Health ©2003 [on line 25.3.2003], URL: http://www.interscience.wiley.com/ullmanns
4. Jelínek L, Parschová H, Matějka Z, Paidar M, Bouzek K (2004) Water Environ Res 76:2686
5. Paidar M, Bouzek K, Jelínek L, Matějka Z (2004) Water Environ Res 76:2691
6. Bouzek K, Paidar M, Sadílková A, Bergmann H (2001) J Appl Electrochem 31:1185
7. Gavagnin R, Biasetto L, Pinna F, Strukul G (2002) Appl Catal B: Environ 38:91
8. Roveda A, Benedetti A, Pinna F, Strukul G (2003) Inorg Chim Acta 349:203
9. Pintar A, Batista J (1999) Catal Today 53:35
10. Prüsse U, Hähnlein M, Daum J, Vorlop K-D (2000) Catal Today 55:79
11. Lemaignen L, Tong C, Begon V, Burch R, Chadwick D (2002) Catal Today 75:43
12. Daub K, Emig G, Chollier M-J, Callant M, Dittmayer R (1999) Chem Eng Sci 54:1577
13. Berndt H, Mönnich I, Lücke B, Menzel M (2001) Appl Catal B: Environ 30:111
14. de Vooys ACA, van Santen RA, van Veen JAR (2000) J Mol Catal A 154:203
15. Gootzen JFE, Lefferts L, van Veen JAR (1999) Appl Catal A: Gen 188:127
16. Shimazu K, Kawaguchi T, Tada K (2002) J Electroanal Chem 529:20
17. Shimazu K, Goto R, Tada K (2002) Chem Lett 31:204
18. Miodownik AP, Saunders N (1990) In: Massalski TB (ed) Binary alloy phase diagrams 2, 2nd edn. ASM International, pp 1481–1483
19. Paidar M, Bouzek K, Bergmann H (2002) Chem Eng J 85:99
20. Shams El Din AM, Abd El Wahab FM (1965) Electrochim Acta 10:1127